Performance Analysis and Constellation Optimization of Star-QAM-Aided Differential Faster-than-Nyquist Signaling

Chie Sagayama, *Student Member, IEEE*, Takumi Ishihara, *Student Member, IEEE*, and Shinya Sugiura, *Senior Member, IEEE*

***Abstract*—In this letter, motivated by the recent differential faster-than-Nyquist (DFTN) signaling concept, we propose an improved 16-point double-ring star quadrature amplitude modulation (QAM)-aided DFTN signaling transmission, which allows us to attain a higher bandwidth efficiency as well as a simple receiver based on noncoherent detection. We derive an analytical error-rate bound for the proposed star-QAM DFTN signaling in an uncoded scenario. The derived bound is used for optimizing the star-QAM constellation for our DFTN signaling in terms of error-rate performance in an uncoded scenario. Our simulation results demonstrate that the proposed star-QAM DFTN scheme outperforms its conventional phase-shift-keying-based DFTN counterpart.**

I. Introduction

THE concept of faster-than-Nyquist (FTN) signaling was discovered in the 1970s [1, 2] and acts as a means of increasing a transmission rate without expanding the bandwidth. The symbol interval of FTN signaling T is set to a value less than the first Nyquist criterion T_0. One of the main limitations imposed on FTN signaling is that the receiver suffers from inter-symbol interference (ISI), which is specific to FTN signaling. In order to combat this limitation, several computationally efficient frequency-domain equalizers have been developed [3–6], all of which rely on cyclic prefix (CP)-assisted frequency-domain equalization (FDE), which achieve a practically low detection complexity even in a highly dispersive frequency-selective channel, in addition to FTN-induced ISI.

In order to reduce the pilot overhead associated with channel estimation at the receiver, an FTN pilot (FTNP) sequence was employed in [6, 7], where efficient FTNP-based channel estimation (CE) algorithms were developed in the frequency domain. However, the benefit of such reduced pilot overhead is achieved at the cost of additional complexity, which is imposed by the iterative process at the receiver. More specifically, the FTNP-based CE schemes [6, 7] still rely on the use of pilot symbols. Most recently, in order to dispense with CE at the receiver, differential FTN (DFTN) signaling was proposed in [8], where differential phase-shift keying (DPSK) is employed in the context of the conventional FTN signaling. Although in general, noncoherent detection is possible only for an ISI-free non-dispersive channel, noncoherent detection of ISI-contaminated DFTN signaling becomes realistic in [8], by exploiting the fact that an FTN-specific ISI matrix is known in advance of transmissions at the receiver.

The conventional differential star-quadrature amplitude modulation (QAM) scheme typically exhibits a better performance than the DPSK scheme [9, 10], and hence a similar benefit is also expected in the DFTN signaling scenario. However, it is an open issue to optimize a constellation of star-QAM in DFTN signaling, unlike in the conventional Nyquist-criterion-based scenario [9, 10]. This is because the optimum star-QAM constellation in DFTN signaling may depend on the bit-energy-to-noise ratio ($\mathrm{E}_b/\mathrm{N}_0$) as well as the DFTN-specific symbol packing ratio $\alpha = T/T_0$.

Against the above-mentioned backcloth, the novel contributions of this letter are as follows. We first propose an improved DFTN signaling based on 16-point star-QAM in order to enhance the bandwidth efficiency of the conventional BPSK-modulated DFTN signaling scheme [8] while maintaining the DFTN scheme's fundamental benefits. We derive the analytical error-rate bound of the proposed 16-point star-QAM-aided DFTN signaling scheme in an uncoded scenario. The derived bound is exploited for optimizing the 16-point star-QAM constellation in the proposed scheme. Our analytical and numerical results demonstrate that the above-mentioned fundamental benefits of the proposed star-QAM-aided DFTN signaling are achievable. Furthermore, it is found that our scheme exhibits an explicit advantage over the existing coherent counterpart, especially in a rapidly time-varying channel.

II. System Model of Star-QAM-Aided DFTN

In this section, we present the system models of the conventional Nyquist-criterion star-QAM-aided differential modulation and our star-QAM-aided DFTN signaling. In this letter, we consider a double-ring star-QAM having a constellation size of 16, similar to [11]. The amplitudes of the inner and outer rings are denoted by a_L and a_H, and $\gamma = a_H/a_L$ is referred to as the ring ratio.

A. The Conventional Star-QAM-Aided Differential Modulation [10]

We first review the conventional star-QAM-aided differential modulation. At the transmitter, a $4N$-length bit sequence $\mathbf{b} = [b_1, \cdots, b_{4N}]^T \in \mathbb{Z}^{4N}$ per block is differentially modulated onto 16-star-QAM symbols $\mathbf{s} = [s_0, \cdots, s_N]^T \in \mathbb{C}^{N+1}$ as follows:

$$s_k = a_k v_k \quad \text{for} \quad 1 \leq k \leq N, \tag{1}$$

where $a_k \in \{a_H, a_L\}$ is the amplitude of s_k, which is modulated by b_{4k}. For example, we have $a_k = a_L$ for $b_{4k} = 0$, and otherwise we have $a_k = a_H$.

C. Sagayama and T. Ishihara are with the Department of Computer and Information Sciences, Tokyo University of Agriculture and Technology, Kogani, Tokyo 184-8588, Japan. S. Sugiura is with the Institute of Industrial Science, University of Tokyo, Meguro-ku, Tokyo 153-8505, Japan (e-mail: sugiura@ieee.org). *(Corresponding author: Shinya Sugiura.)*

Furthermore, v_k ($|v_k| = 1$) corresponds to a differentially modulated phase of s_k, which is given by

$$v_k = w_k v_{k-1}, \tag{2}$$

and w_k is an 8-PSK symbol, which is modulated based on three bits, i.e., $[b_{4k-3}, b_{4k-2}, b_{4k-1}]$. Note that the initial amplitude and 8-PSK symbol are set to $a_0 = a_L$ and $v_0 = 1$, respectively.

The differentially encoded star-QAM signals are transmitted to the receiver over a frequency-flat Rayleigh fading channel. The received symbols $y_k \in \mathbb{C}$ $(k = 0, \cdots, N)$ is expressed as follows:

$$y_k = h_k s_k + n_k = h_k a_k v_k + n_k, \tag{3}$$

where $h_k \in \mathbb{C}$ is the channel coefficient, and $n_k \in \mathbb{C}$ is the associated additive white Gaussian noise (AWGN) component, which obeys a complex-valued Gaussian distribution having a zero mean and a noise variance of N_0. By assuming that two consecutive channel coefficients remain constant, i.e., $h_k = h_{k-1}$, the received signals y_k of (3) are rewritten as

$$y_k = h_{k-1} a_k v_{k-1} w_k + n_k = \frac{a_k}{a_{k-1}} y_{k-1} w_k + \tilde{n}_k, \tag{4}$$

where we have an equivalent noise component of $\tilde{n}_k = -(a_k/a_{k-1}) n_{k-1} w_k + n_k$, which obeys a complex-valued Gaussian distribution having a zero mean and a variance of $\{(a_k/a_{k-1})^2 + 1\} N_0$. Note that a_k/a_{k-1} of (4) has value 1, γ, or $1/\gamma$.

Having obtained the modified received signal model of (4), four information bits $[b_{4k-3}, b_{4k-2}, b_{4k-1}, b_{4k}]$ are estimated by demodulating (a_k, w_k) without channel estimation, based on the maximum likelihood (ML) criterion, as follows: [12]

$$(\hat{a}_k, \hat{w}_k) = \arg\max_{(a_k, w_k)} \left\{ \frac{|a_k w_k^* + \hat{a}_{k-1} \hat{w}_{k-1}^*|^2}{|a_k|^2 + |\hat{a}_{k-1}|^2} - \left(|w_k|^2 + |\hat{w}_{k-1}|^2 \right) \right\}, \tag{5}$$

where $\hat{a}_k$ and $\hat{w}_k$ are the estimated amplitude and phase, a_k is a_L or a_H, and w is an 8-PSK symbol and the equation holds when E_b/N_0 is fully large [12].

B. The Proposed Star-QAM-Aided DFTN Signaling

In the proposed transmitter, similar to the conventional differential 16-star-QAM in Section II-A, $4N$ information bits are modulated onto $(N+1)$-length differential 16-star-QAM symbols $\mathbf{s}$. Then, a 2ν-length CP is added to the head of $\mathbf{s}$, in order to obtain $(N + 2\nu + 1)$-length symbols $\tilde{\mathbf{s}} \in \mathbb{C}^{N+2\nu+1}$. Note that ν is assumed to be sufficiently longer than the effective tap length induced by DFTN signaling. Here, the effective tap length includes both the ISI effects, induced by the FTN signaling and the frequency-flat channels, similar to [13]. Then, the transmitted signals $\tilde{s}(t)$ are generated by band-limiting $\tilde{\mathbf{s}}$ with the aid of an root raised cosine (RRC) filter $q(t)$ having a roll-off factor of β, as follows:

$$\tilde{s}(t) = \sum_n \tilde{s}_n q(t - nT). \tag{6}$$

Note that in this model, the E_b/N_0 of the DFTN signaling is the same as that of the conventional Nyquist-criterion-based counterpart. By assuming a quasi-static frequency-flat Rayleigh fading channel, the kth sampled symbol z_k at the receiver is given by

$$z_k = h \sum_n \tilde{s}_n g((k-n)T) + \eta(kT), \tag{7}$$

where we have $g(t) = \int q(\tau) q^*(\tau - t) d\tau$ and $\eta(t) = \int n(t) q^*(\tau - t) d\tau$. Additionally, $\eta(kT)$ $(k = 0, \cdots, N + 2\nu)$ are the colored noise components, which have the relationship $\mathbb{E}[\eta(kT)\eta(jT)] = N_0 g((k-j)T)$. Here, $\mathbb{E}[\cdot]$ denotes the expectation operation.

Furthermore, by removing both the ν head and the last ν symbols from the $N + 2\nu + 1$ sampled symbol block, the received block is obtained as follows:

$$\hat{\mathbf{y}} = h\mathbf{G}\mathbf{s} + \boldsymbol{\eta}, \tag{8}$$

where $\mathbf{G} \in \mathbb{R}^{(N+1)\times(N+1)}$ is a circulant matrix that corresponds to the FTN-specific ISI effects. Moreover, $\mathbf{G}$ is expressed by $\mathbf{G} = \mathbf{Q}^{\mathbf{T}} \mathbf{\Lambda} \mathbf{Q}^*$ with the aid of the eigenvalue decomposition, where $\mathbf{Q}$ is a normalized discrete Fourier transform (DFT) matrix whose kth row and lth column component is $(1/\sqrt{N+1}) \exp[-2\pi j(l-1)(k-1)/(N+1)]$. Hence, by carrying out an inverse DFT operation on (4), we arrive at the frequency-domain received signals of

$$\begin{aligned} \hat{\mathbf{y}}_f &= \mathbf{Q}^* \hat{\mathbf{y}} \\ &= h\mathbf{\Lambda}\mathbf{Q}^*\mathbf{s} + \mathbf{Q}^*\boldsymbol{\eta}. \end{aligned} \tag{9}$$

Since the FTN-specific ISI matrix $\mathbf{G}$ is calculated by the symbol packing ratio α and the roll-off factor of an RRC filter β, $\mathbf{G}$ is accurately available at the receiver, versus requiring estimation.

With the aid of the approximated noise-whitening minimum mean-square error (MMSE) criterion [6], the estimates of $\mathbf{z} = h\mathbf{s}$ are calculated as follows:

$$\hat{\mathbf{z}} = [\hat{z}_0, \cdots, \hat{z}_N]^T \in \mathbb{C}^{N+1} \tag{10}$$

$$= \mathbf{Q}^T \mathbf{W} \hat{\mathbf{y}}_f, \tag{11}$$

where we have

$$\mathbf{W} = \mathbf{\Lambda}^H \left(\mathbf{\Lambda}\mathbf{\Lambda}^H + \frac{N_0}{E_s} \mathbf{\Phi}_\eta \right)^{-1}, \tag{12}$$

and E_s represents the symbol power. Furthermore, $\mathbf{\Phi}_\eta = \mathrm{diag}\left(\Phi_\eta[0], \cdots, \Phi_\eta[N]\right)$ is a diagonal matrix whose nth element is

$$\Phi_\eta[n] = \frac{1}{N+1} \sum_{l=0}^{N} \sum_{m=0}^{N} g((l-m)T) \exp\left(j \frac{2\pi(l-m)n}{N+1} \right) \quad (0 \le n \le N). \tag{13}$$

Finally, by substituting $\hat{z}_k$ and $\hat{z}_{k-1}$ in (11) into y_k and y_{k-1} in (4), the kth symbol $\tilde{s}_k$ is estimated with the aid of ML detection.

III. Analytical Error-Rate Bound

In [8], the equivalent signal-to-interference-pulse-noise ratio (SINR) value of the received DFTN signals after MMSE-based

FDE is derived. In [14], the analytical BER expression of the differentially encoded 16-star-QAM scheme is given. Assisted by these results, we herein derive the analytical error-rate bound of our 16-QAM-aided DFTN signaling scheme.

The estimated 16-star-QAM-aided DFTN symbols $\hat{\mathbf{s}}$ are given by [8]

$$\begin{aligned}\hat{\mathbf{s}} &= h\mathbf{Q}^T\mathbf{W}\mathbf{\Lambda}\mathbf{Q}^*\mathbf{s} + \mathbf{Q}^T\mathbf{W}\mathbf{Q}^*\boldsymbol{\eta} \\ &= h\mathbf{\Gamma_s}\mathbf{s} + \mathbf{\Gamma_n}\boldsymbol{\eta},\end{aligned} \tag{14}$$

where we have $\mathbf{\Gamma_n} = \mathbf{Q}^T\mathbf{W}\mathbf{Q}^*$ and $\mathbf{\Gamma_s} = \mathbf{\Gamma_n}\mathbf{G}$. More specifically, the desired signals, the FTN-specific ISI, and the AWGNs are represented, respectively, by $\mathbf{s}_d = h\mathbf{\Gamma_d}\mathbf{s}$, $\mathbf{s}_I = h(\mathbf{\Gamma_s} - \mathbf{\Gamma_d})\mathbf{s}$, and $\boldsymbol{\eta}_\nu = \mathbf{\Gamma_n}\boldsymbol{\eta}$, where $\mathbf{\Gamma_d}$ is a diagonal matrix having diagonal elements of $\mathbf{\Gamma_s}$. By considering $\mathbb{E}[|h|^2] = 1$ and $\mathbb{E}[\mathbf{s}\mathbf{s}^H] = \mathbf{I}_{N+1}$, the average power of each component is formulated as

$$P_d = \mathrm{tr}\left\{\mathbb{E}[\mathbf{s}_d\mathbf{s}_d^H]\right\} = \mathrm{tr}\left\{\mathbf{\Gamma}_\mathrm{d}\mathbf{\Gamma}_d^H\right\}, \tag{15}$$

$$\begin{aligned}P_I &= \mathrm{tr}\left\{\mathbb{E}[\mathbf{s}_I\mathbf{s}_I^H]\right\} \\ &= \mathrm{tr}\left\{|\mathbf{\Gamma}_\mathrm{s}|^2 + |\mathbf{\Gamma}_\mathrm{d}|^2 - \mathbf{\Gamma}_s\mathbf{\Gamma}_d^H - \mathbf{\Gamma}_d\mathbf{\Gamma}_s^H\right\},\end{aligned} \tag{16}$$

$$P_\eta = \mathrm{tr}\left\{\mathbb{E}[\boldsymbol{\eta}_\nu\boldsymbol{\eta}_\nu^H]\right\} = \mathrm{tr}\left\{\mathbf{\Gamma}_n\mathbf{R}\mathbf{\Gamma}_n^H\right\}, \tag{17}$$

where $\mathbf{R} = \mathbb{E}[\boldsymbol{\eta}\boldsymbol{\eta}^H]$, the ith row and jth column element of which is given by $N_0 g((l-m)T)$. Hence, the average SINR value of DFTN signaling after MMSE-FDE is given by

$$\mathrm{SINR} = \frac{P_d}{P_I + P_\eta}. \tag{18}$$

Differential 16-star-QAM is divided into two differential modulation schemes: two-level differential amplitude shift keying (2-DASK) and 8-DPSK. In [14], in order to detect coherent Nyquist-criterion differentially encoded 16-star-QAM symbols, a thresholding scheme, rather than ML detection, was employed for detecting an amplitude a_k. Two thresholding values are set: $\xi_L = 2/(1+\gamma)$ and $\xi_H = (1+\gamma)/2$. If $\xi_L \le |y_k|/|y_{k-1}| \le \xi_H$, then the amplitude is estimated as $\hat{a}_k = \hat{a}_{k-1}$, that is $b_{4k} = 0$, and otherwise the amplitude is estimated as $\hat{a}_k \neq \hat{a}_{k-1}$, that is $b_{4k} = 1$.

The analytical BER of differential 16-star-QAM is expressed as

$$P_{\text{16starQAM}} = \frac{1}{4}P_{\text{2-DASK}} + \frac{3}{4}P_{\text{8-DPSK}}, \tag{19}$$

where $P_{\text{2-DASK}}$ and $P_{\text{8-DPSK}}$ are the analytical BERs of 2-DASK and 8-DPSK, respectively. Furthermore, letting the amplitude of the nth symbol be c_n, $P_{\text{2-DASK}}$ and $P_{\text{8-DPSK}}$ are formulated as

$$\begin{aligned}P_{\text{2-DASK}} = \frac{1}{2} + \frac{1}{4}\sum_{c_n}\sum_{c_{n-1}}\epsilon(c_n, c_{n-1}) \\ [P(\xi = \xi_H|c_n, c_{n-1}) - P(\xi = \xi_L|c_n, c_{n-1})],\end{aligned} \tag{20}$$

$$P_{\text{8-DPSK}} = \frac{2}{3}\left[F_{\text{8-DPSK}}\left(\psi = -\frac{\pi}{8}\right) - F_{\text{8-DPSK}}\left(\psi = -\frac{3\pi}{8}\right)\right], \tag{21}$$

where

$$\epsilon(c_n, c_{n-1}) = \begin{cases} 1 & (c_n \neq c_{n-1}) \\ -1 & (c_n = c_{n-1}). \end{cases} \tag{22}$$

$$P(\xi \,|\, c_n, c_{n-1}) = \frac{1}{2}\left\{1 + \frac{\xi^2 - \rho_2^2/\rho_1^2}{\sqrt{(\xi^2 + \sigma_2^2/\sigma_1^2) - (2\xi\sigma_2/\sigma_1)^2}}\right\}, \tag{23}$$

$$\begin{aligned}F_{\text{8-DPSK}}(\psi) = \frac{1}{2}\Bigg[1 + \frac{\psi}{\pi} + \frac{2}{\pi}\frac{\rho\sin\psi}{\sqrt{1-\rho^2\cos^2\psi}} \\ \times \tan^{-1}\sqrt{\frac{1+\rho\cos\psi}{1-\rho\cos\psi}}\Bigg].\end{aligned} \tag{24}$$

Furthermore, we have $\sigma_2^2/\sigma_1^2 = (c_n^2 + 1/\Gamma)$, $\rho = c_n c_{n-1}/[(c_{n-1}^2 + 1/\Gamma)(c_n^2 + 1/\Gamma)]^{1/2}$, and Γ is the average SINR value. Finally, the analytical BER of our proposed differential 16-star-QAM-aided DFTN signaling is obtained by substituting the SINR of (18) into Γ of (19)–(24).

IV. Performance Results

In this section, we provide our performance results for 16-star-QAM-aided DFTN signaling. The basic parameters employed in our simulations are as follows. The block length of DFTN symbols was set to $N = 1024$, and a frequency-flat Rayleigh fading channel was assumed. The roll-off factor of the RRC filter was maintained as β =0.3, and the CP length was assumed to be $2\nu = 20$. Note that the constellation has to be optimized, depending on the roll-off factor β employed. Furthermore, ML detection was employed to calculate the simulated BER curves of the proposed DFTN signaling scheme.

Based on the derived analytical bound of the proposed DFTN signaling, we optimized the ring ratio γ for each symbol packing ratio α. We assumed the use of the thresholding parameters $\xi_L = 2/(1+\gamma)$ and $\xi_H = (1+\gamma)/2$, according to [11]. Fig. 1(a) shows the relationship between ring ratio γ and the BERs for an E_b/N_0 of 20 dB. Symbol packing ratio α was set to 0.7, 0.8, 0.9, or 1.0. Observe in Fig. 1(a) that the optimum ring ratio γ changed, depending on symbol packing ratio α. Furthermore, in Fig. 1(b), the optimum ring ratios γ for symbol packing ratios of $\alpha = 0.7$, 0.8, 0.9, and 1.0 were plotted. As seen in Fig. 1(b), for the low E_b/N_0s, the optimum ring ratios change depending on symbol packing ratio α. For the high E_b/N_0s, such as $E_b/N_0 > 40$ dB, the optimum ring ratio converges to $\gamma = 2.09$ regardless of the α value. Note that in the range of $\alpha < 0.8$, the accuracy of the analytical BER decreases, upon decreasing the α value, similar to [8].

In Fig. 2, we show the numerical results of the achievable BER performance in the AWGN channel comparing the proposed 16-star-QAM-aided DFTN scheme, the 16-star-QAM-aided FTN scheme, the conventional 16-PSK-aided DFTN scheme, and the conventional 16-PSK-aided FTN scheme. Moreover, the ring ratio of 16-star-QAM was fixed to $\gamma = 2.1$, and the symbol packing ratio was set as $\alpha = 0.9$ or 0.8. Observe in Fig. 2 that the proposed 16-star-QAM-aided DFTN signaling scheme exhibited a 3-dB penalty over its coherent counterpart, as expected. This is due to the noise-doubling effects, which specifically depend on ring ratio γ. Also, the

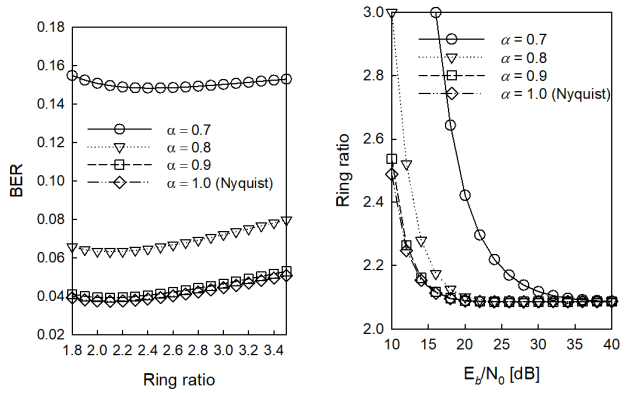

(a) BER at $E_b/N_0 = 20$ dB (b) Optimum ring ratio

Fig. 1. Achievable BER performance and optimum ring ratio γ of the proposed 16-point star-QAM-aided DFTN signaling. A time-invariant frequency-flat Rayleigh fading channel was considered; α is the symbol packing ratio. (a) Achievable BER at the E_b/N_0 of 20 dB for each α value; (b) ring ratio optimized at each E_b/N_0.

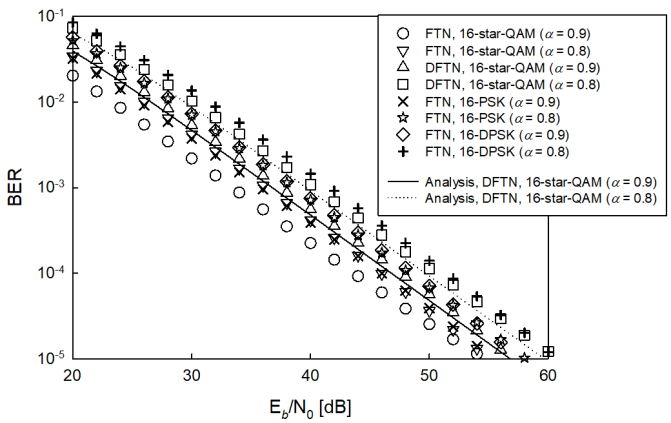

Fig. 2. Achievable BER performance of the coherent FTN and DFTN schemes, which were modulated based on 16-star-QAM and 16-PSK. An AWGN channel was considered; α is the symbol packing ratio.

proposed 16-star-QAM-aided DFTN signaling scheme outperformed the conventional 16-PSK-aided DFTN one in terms of BER. Note that the performance gain owing to the constellation optimization is on the order of a fraction of dB. However, this is not marginal from the physical-layer perspective, since this optimization can be carried out offline [15].

The above performance results assumed time-invariant channels; next we investigate the effects of using time-varying channels. In the time-varying scenario, the received signals of (7) are modified to $z_k = \sum_n h_n s_n g(k-nT) + \eta(kT)$, where h_n $(n = 0, \cdots, N+2\nu+1)$ is the channel coefficient at the nth sample, which is generated according to $\mathbb{E}[h_n h^*_{n+\tau}] = J_0(2\pi F_d T \tau)$, in which $F_d T$ is the normalized Doppler frequency and J_0 is the zero-order Bessel function of the first kind. We assumed that, for coherent FTN schemes, the channel coefficient was updated at the beginning of each

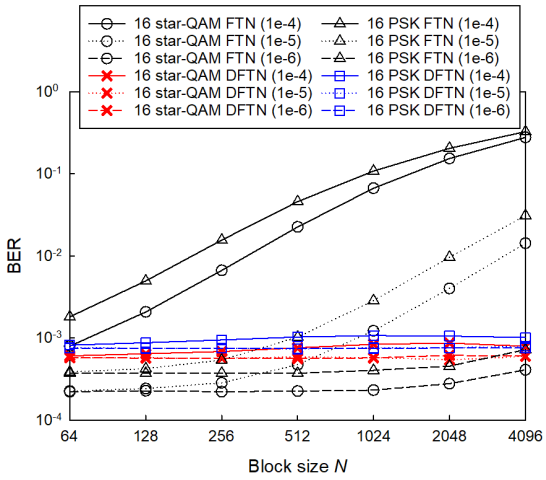

Fig. 3. Achievable BERs for the coherent FTN and DFTN signaling schemes modulated based on 16-star-QAM and 16 PSK. A time-varying frequency-flat Rayleigh fading channel was considered at an E_b/N_0 of 40 dB. The symbol packing ratio was set as $\alpha = 0.9$, and the normalized Doppler frequency (given in parentheses in the legend key) was set as $F_d T_s = 1.0 \times 10^{-6}$, 1.0×10^{-5}, or 1.0×10^{-4}.

block.[1]

Finally, as shown in Fig. 3, the effects of a block length on the achievable BER performance in a time-varying channel were investigated while considering an E_b/N_0 of 40 dB. Also, the block length N was varied from 2^6 to 2^{12}, while the number of CP was maintained as $2\nu = 20$. The symbol packing ratio was set as $\alpha = 0.9$ and the maximum Doppler frequency was given by 1×10^{-4}, 1×10^{-5}, and 1×10^{-6}. Observe in Fig. 3 that the BERs of the proposed 16-star-QAM-aided DFTN signaling scheme remained unchanged regardless of the block length, while those of the coherent counterpart deteriorated upon increasing the block length.[2][3]

V. Conclusions

In this letter, we proposed a novel 16-point star-QAM-aided DFTN signaling scheme in order to achieve a better bandwidth efficiency without the pilot overhead associated with channel estimation. The analytical error-rate bound was derived based on the equivalent SINR value for an MMSE-FDE-aided receiver. Furthermore, using this derived bound, a 16-point star-QAM constellation was optimized for our DFTN signaling scheme in terms of the error-rate performance. Our performance results revealed that the proposed DFTN scheme achieved enhanced performance relative to the conventional 16-PSK-modulated DFTN scheme, as well as outperforming its coherent counterparts, especially in a rapidly time-varying channel.

[1]To expound a little further, for the sake of operating with a low α value, such as $\alpha < 0.8$, in the DFTN and FTN schemes, the use of powerful channel-coding scheme is needed, as mentioned in [6, 13].

[2]Note that the proposed DFTN scheme is not directly applicable to the frequency-selective channel, similar to the conventional differentially-modulated systems.

[3]Note that while our DFTN scheme was optimized for the quasi-static channel, that employing the same parameters exhibited a good BER performance in the time-varying channel.

REFERENCES

[1] J. Salz, "Optimum mean-square decision feedback equalization," *Bell System Technical Journal*, vol. 52, no. 8, pp. 1341–1373, 1973.

[2] J. Mazo, "Faster-than-Nyquist signaling," *Bell System Technical Journal*, vol. 54, no. 8, pp. 1451–1462, 1975.

[3] S. Sugiura, "Frequency-domain equalization of faster-than-Nyquist signaling," *IEEE Wireless Communications Letters*, vol. 2, no. 5, pp. 555–558, Oct. 2013.

[4] R. Dinis, B. Cunha, F. Ganhao, L. Bernardo, R. Oliveira, and P. Pinto, "A hybrid ARQ scheme for faster than Nyquist signaling with iterative frequency-domain detection," in *IEEE 81st Vehicular Technology Conference (VTC2015-Spring)*, May 2015, pp. 1–5.

[5] W. Yuan, N. Wu, H. Wang, and J. Kuang, "Variational inference-based frequency-domain equalization for faster-than-Nyquist signaling in doubly selective channels," *IEEE Signal Processing Letters*, vol. 23, no. 9, pp. 1270–1274, Sept. 2016.

[6] T. Ishihara and S. Sugiura, "Iterative frequency-domain joint channel estimation and data detection of faster-than-Nyquist signaling," *IEEE Transactions on Wireless Communications*, vol. 16, no. 9, pp. 6221–6231, Sept. 2017.

[7] Q. Shi, N. Wu, X. Ma, and H. Wang, "Frequency-domain joint channel estimation and decoding for faster-than-Nyquist signaling," *IEEE Transactions on Communications*, 2017, in press.

[8] T. Ishihara and S. Sugiura, "Differential faster-than-Nyquist signaling," *IEEE Access*, vol. 6, pp. 4199–4206, 2018.

[9] C.-D. Chung, "Differentially amplitude and phase-encoded QAM for the correlated rayleigh-fading channel with diversity reception," *IEEE Transactions on Communications*, vol. 45, no. 3, pp. 309–321, Mar. 1997.

[10] D. Liang, S. X. Ng, and L. Hanzo, "Soft-decision star-QAM aided BICM-ID," *IEEE Signal Processing Letters*, vol. 18, no. 3, pp. 169–172, Mar. 2011.

[11] W. T. Webb, L. Hanzo, and R. Steele, "Bandwidth efficient QAM schemes for Rayleigh fading channels," *IEE Proceedings I - Communications, Speech and Vision*, vol. 138, no. 3, pp. 169–175, June 1991.

[12] T. Suzuki and T. Mizuno, "Multiple-symbol differential detection scheme for differential amplitude modulation," in *Mobile Communications Advanced Systems and Components*, C. G. Günther, Ed. Berlin, Heidelberg: Springer Berlin Heidelberg, 1994, pp. 196–207.

[13] S. Sugiura and L. Hanzo, "Frequency-domain-equalization-aided iterative detection of faster-than-Nyquist signaling," *IEEE Transactions on Vehicular Technology*, vol. 64, no. 5, pp. 2122–2128, 2015.

[14] F. Adachi and M. Sawahashi, "Performance analysis of various 16 level modulation schemes under Rayleigh fading," *Electronics Letters*, vol. 28, no. 17, pp. 1579–1581, 1992.

[15] S. Sugiura and L. Hanzo, "On the joint optimization of dispersion matrices and constellations for near-capacity irregular precoded space-time shift keying," *IEEE Transactions on Wireless Communications*, vol. 12, no. 1, pp. 380–387, Jan. 2013.